# CHATTERING REDUCTION IN DOUBLY FED INDUCTION GENERATORS USING SECOND ORDER SLIDING MODE CONTROL SCHEMES

S.F. Anas[1] & A. S. Abubakar[2]
Department of Electrical Engineering, Ahmadu Bello University Zaria, Nigeria
*anasshfa@gmail.com, [2]abubakaras@abu.edu.ng,

**Keywords: –**
*Doubly-fed induction generator.*
*Sliding Mode Control.*
*Second-Order Sliding Mode.*
*Wind Turbine.*
.

**Article History: –**
**Received:** April, 2020.
**Reviewed:** May, 2020
**Accepted:** July, 2020
**Published:** September, 2020

**ABSTRACT**

*Wind farm are gaining attention in the present-day power industries. It employs the use of Induction Generator (IG) with multiple variations and operation. The concept of variations in pitch and speed respectively to control WT is referred to as Doubly-fed Induction Generator (DFIG). Though, DFIGs are highly susceptible to instabilities. To address these issues, a sliding mode control (SMC) scheme for a grid-connected wind turbine WT is proposed to alleviate DFIGs susceptibility. Although SMCs have a major setback of chattering. Second-order sliding mode (SOSM) control is presented to effectively mitigate the chattering effect along the switching surface. Also, the scheme employs control laws to ensure chattering free implementation of SOSM. The control scheme was designed to exploit high wind penetration from the wind farm and ensure a maximum reduction in overshoot. The systematic design approach of SOSM is presented, performance evaluation between the controller was carried out. The work was implemented on a DFIG model, and complete simulation of the system was carried out in MATLAB/Simulink_R2018a environment. The result obtained was compared with a PI controller to show the effectiveness of the control strategy.*

## 1. INTRODUCTION

In recent years, growing concern in the research community towards a sustainable environment has led a quest for clean and pure energy [5]. Alternative resources which include wind, tidal wave, solar, geothermal are attracting more attention to satisfying societies' power demand. [3]. Power generating countries prefer Renewable Energy Sources (RES) and wind energy falls among the cleanest RES is, highly favored [14]. Wind power generation has accomplished an exponential progress in the last few years [5], representing 3.5% of worldwide energy consumption [14]. The rapid integration of wind power in comparison to different RES have turn out to be a vital element within the modern power network [14]. Wind power employing DFIG has numerous advantages which includes; variable speed operation, efficiency and 4 quadrant operation in comparison to squirrel cage induction generator (SCIG), wound rotor induction generator (WRIG) and permanent magnet synchronous generator (PMSG) [4]. In DFIG, stator and rotor are connected to the grid respectively, only that the rotor is coupled with bidirectional converter. The function of the converter is to control the active and reactive power between the stator and ac supply [15]. The contemporary trend regarding wind energy is to preserve and maintain the growth all through the next decade. In this day and age, installation of powerfully and reliable WT in windier zones is becoming a challenge [11]. Wind farm possess non-linear dynamics and uncertainties. As a result, the rotor position angle, mutual inductance between the stator and rotor have non-linear characteristic in DFIG respectively [11]. To avoid these drawbacks, Sliding Mode Control (SMC) control technique was proposed to alleviate the setback. SMC is a non-linear control technique with better tracking ability as well as compensating disturbances in systems [1]. However, chattering has been a major setback in most systems with SMCs. Chattering causes high mechanical stress, together with poor control accuracy [6]. Second-order sliding mode (SOSM) is therefore proposed to mitigate the chattering effect in SMCs. In [6], a robust-fractional order sliding mode controller for MPPT of DFIG based WECS was used, but chattering effect was acknowledged as a result of an error in uncertainty

estimator in the work. [12] uses a back-stepping control approach for the rotor and grid side converters of DFIG. The model responds very fast in low wind speed penetration with high overshoot, and on the contrary, it responds slowly as acknowledge in the work on high wind speed penetration with a significant decrease in overshoot. [8] worked on various control schemes of the WEC system aiming at good performance despite external disturbances. The work suffered from the power converter used in PMSG as it encores power losses and generates a substantial rate of harmonics. [16] uses fixed gain super twisting mode to design. The work choose error in electromagnetic torque and reactive power respectively as their sliding variables. It was however, affected by chattering, as acknowledged in their work. Therefore, this work proposed a control strategy to mitigate the chattering effect in sliding mode control systems.

## 2.0 SYSTEM MODELLING

Since the installation of the first WT system in the early 1980s, the use of DFIG in the grid is rapidly progressing. This innovation in the WT system has made the use of DFIG more attractive due to its ability to provide continuous power supply to the grid and adapt with wind speed variation [13]. Figure 1 shows a grid connected DFIG.

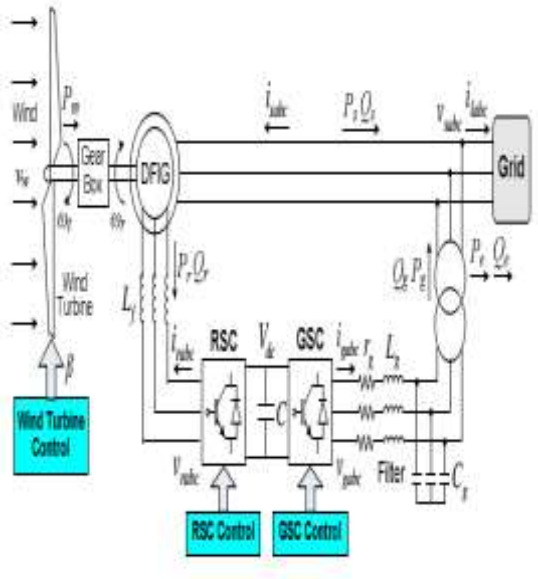


Figure 1: Grid-Connected DFIG [14]

### 2.1 Model of Doubly Fed Induction Generator

To model a DFIG, the dynamic equations can be described using the equations governing induction machines [10]. A DFIG is simply a normal wound rotor induction machine having the stator terminals connected directly to the grid. The rotor winding is connected via power electronic converter to grid [14]. The following Figure 2 is valid for an equivalent Y phase and for steady-state calculations respectively. if the DFIG is a delta-connected, the machine can be represented by the circuit [10].

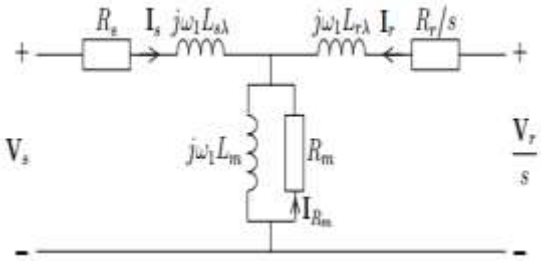


Figure 2: Equivalent Circuit of DFIG

Under ideal condition and applying the Kirchhoff's voltage law to Figure 2,

$$V_s = R_s I_s + j\omega_1 L_{s\lambda} I_s + j\omega_1 L_m (I_s + I_r + I_{Rm}) \quad (1)$$

$$\frac{V_r}{s} = \frac{R_r}{s} I_r + j\omega_1 L_{r\lambda} I_s + j\omega_1 L_m (I_s + I_r + I_{Rm}) \quad (2)$$

$$0 = R_m I_{Rm} + j\omega_1 L_m (I_s + I_r + I_{Rm}) \quad (3)$$

Where $V_s$ & $V_r$ : stator and rotor voltage

$R_s$ & $R_r$ : stator and rotor resistance respectively

$I_s$ & $I_r$ : stator and rotor current respectively

$L_{s\lambda}$ & $L_{r\lambda}$ : stator and rotor leakage inductance respectively

$\omega_1$ : stator frequency

$R_m$ : magnetizing resistance

$I_{Rm}$ : magnetizing resistance current

$L_m$ : magnetizing inductance

$s$ : slip

Furthermore, if the stator flux, rotor flux and the air-gap flux are defined as

$$\psi_s = L_{s\lambda}I_s + L_m(I_s + I_r + I_{Rm}) = L_{s\lambda}I_s + \psi_m \quad (4)$$

$$\psi_r = L_{r\lambda}I_r + L_m(I_s + I_r + I_{Rm}) = L_{r\lambda}I_r + \psi_m \quad (5)$$

$$\psi_m = L_m(I_s + I_r + I_{Rm}) \quad (6)$$

Therefore, equation (1) - (3), which describe the equivalent circuit can, be rewritten as

$$\boldsymbol{V_s = R_s I_s + j\omega_1 \psi_s} \quad (7)$$

$$\frac{V_r}{s} = \frac{R_r}{s} I_r + j\omega_1 \psi_r \quad (8)$$

$$0 = R_m I_{Rm} + j\omega_1 \psi_m \quad (9)$$

The equations which describes the electro-mechanical torque $T_e$ is given as

$$T_e = 3n_p I_m[\psi_s I_r] \approx -3n_p \psi_s i_{Rq} \quad (10)$$

Where $T_e$; electromechanical torque

$n_p$;a number of poles

$\psi_s$; stator flux

$i_{Rq}$; rotor current of q-component.

$I_m$; magnetizing current

$I_r$; rotor current

and the resistive losses for the induction generator is express as

$$P_{loss} = 3(R_s|I_s|^2 + R_r|I_r|^2 + R_m|I_{Rm}|^2) \quad (11)$$

### 2.1 Component of Wind Turbine

Wind turbines consist of many subsystems which need a proper consideration when deriving their dynamic models. Some of the models are; the generator, flexible drivetrain, wind, pitch, aerodynamic, flexible tower, nacelle yaw, and torque [7].

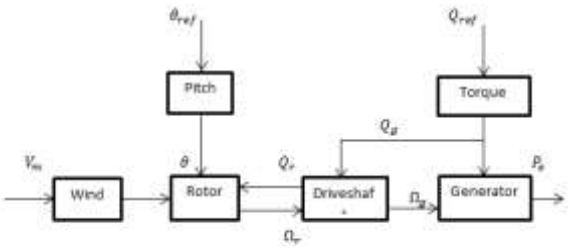


Figure 3. Component of DFIG Wind Energy Conversion System [7]

Figure 3 highlights the basic component of a WEC system. The two inputs to WECS are the generator torque $T_g$ and the blade pitch $\theta$. The mean wind speed is labeled as $V_m$, The aerodynamic torque and generator speed are $T_e$ and $\Omega_g$ respectively. The rotor speed $\Omega_r$ and electric power $P_e$ are the output, respectively [7].

### 2.2 Wind Speed Model

The wind is described as complex due to its varying properties [7] like climate change, weather and land roughness [2]. These properties label wind as a concentrate of two varying frequencies as in (12)

$$V_e(t) = V_m(t) + V_t(t) \quad (12)$$

Thus slow varying mean wind speed and fast varying turbulent wind speed is the model adopted used for two-time scale in simulating the wind speed [8]. The $V_m(t)$ component of (12) can be obtained as (13)

$$V_m(t) = v_0 + \sum_{i=1}^{N} A_i \cos(\omega_i t + \varphi_i) \quad (13)$$

$$A_i = \frac{2}{\pi}\sqrt{\frac{1}{2}(S_{vv}(\omega_i) + S_{vv}(\omega_{i+1})).(\omega_{i+1} - \omega_i)} \quad (14)$$

### 2.3 Aerodynamic Model

The model represents the power extraction of the rotor by determining the mechanical torque which is known to be a function of airflow incident on the blade [16]. It is derived based on the force and kinetic energy of the wind, which gives

$$C_p P_w = \frac{1}{2} C_p(\lambda, \beta)\rho S V^3 \quad (15)$$

Where; $\rho$: is the air density ($^{k_g}/_{m^3}$)

R: radius (m)

$C_p$: power coefficient

$\lambda$: Tip speed ratio

V: wind speed(m/s)

$\beta$: pitch angle

Power coefficient $C_p$ is the representation between wind power and aerodynamic power, which are all linked with blade pitch $\beta$ and tip speed ratio[1]. The following gives an expression of tip speed ratio as

$$\lambda = \frac{\Omega R}{V} \tag{16}$$

The WT control is made such that it extracts maximum power available. The efficiency in extracting wind power is narrowed down to the Betz limit and power coefficient. According to Betz theory, the theoretical maximum efficiency for a WT system cannot exceed 59.3% as it is the best any conventional WT can use its kinetic energy to spin the turbine and generate electricity [8].

$$C_p = 0.5\left(\frac{151}{\lambda_i} - 0.58\beta - 0.002\beta^{2.14} - 10\right)^{-\frac{18.4}{\lambda_i}} e \tag{17}$$

$$\lambda_i = \frac{1}{\frac{1}{\lambda - 0.002\beta} - \frac{0.003}{\beta^3 + 1}} \tag{18}$$

## 3.0 SLIDING MODE CONTROL DESIGN AND STABILITY ANALYSIS

Studies has shown that non-linear control for WECS is gaining attention since most of real systems are basically non-linear. However, linear control methods are remarkable however, it suffers from limited operating ranges [9]. The distinct features of SMC are that the control law is designed such that it drives system trajectory to reach and remain on manifold within the state-space called sliding manifold [8]. The error trajectory after initial reaching phase slides on the manifold $\sigma(e,t) = 0$. SMC is attractive in robust control due to its insensitivity to parametric, and it matched disturbance together with uncertainties [16]. The design for sliding manifold in the second-order actuated system is as

$$\sigma(e,t) = C^T e \tag{19}$$

given that $e \triangleq [e_1\ \dot{e}_2]^T = [e_1\ e_2]^T$ is the error vector and $C^T$ is the sliding manifold parameter vector, which characterizes the manifold. The Position error $e_1$ is defined by $e_1 = x_1 - x_1^d$ and the velocity error $e_2$ is defined as $e_2 = x_2 - x_2^d$. The variable representing the real system trajectories $x_1\ and\ x_2$ with the desired trajectories are $x_1^d\ and\ x_2^d$ respectively. $C^T = [C_1\ \ 1\ ]^T$ without loss of generality. Therefore, (19) and its time-derivatives are given,

$$\sigma(e,t) = C_1\ (x_1 - x_1^d) + (x_2 - x_2^d\ ) \tag{20}$$

$$\dot{\sigma}(e,t) = C_1\ \left(\dot{x_1} - \dot{x_2^d}\right) + \left(\dot{x_2} - \dot{x_2^d}\right) \tag{21}$$

### 3.1 Control design

For experimental WT, the drive train model can be presented in a single lumped as

$$\frac{d_{wr}}{dt} = \frac{1}{j}\left(T_r - K_{wr} - T_g\right) \tag{22}$$

Where $J = J_r + n^2 J_g$

$$K = K_r + n^2 K$$

Now consider the drive train model, which is represented as

$$\dot{\omega}_r(t) = A\omega_r(t) - BT_g(t) + d(t) \tag{23}$$

Given that $T_g$: input command

A: $^K/_J\ and\ B$: $^1/_J$: turbine rotor parameter

$d$: $^{T_r}/_J$ : turbine torque;

It is good to note that the controller is tracking the speed reference as

$$e(t) = \omega_r(t) - \omega_{ref}(t) = 0 \tag{24}$$

Where $\omega_{ref}$: speed reference

$e$: speed tracking error

The dynamic of the tracking error for speed is given as;

$$\dot{e} = \dot{\omega}_r - \dot{\omega}_{ref}$$

$$= -Ae - BT_g + d - \dot{\omega}_{ref}$$

$$= -Ae + u + d \quad (25)$$

$$d^*(t) = -\Delta A\omega_r(t) - \Delta BT_g(t) + d(t) + \zeta(t) \quad (31)$$

The term $d^*$ is a new perturbation that includes any external disturbances, parametric uncertainties and Now, the new control input $u$ is given by

$$u = -BT_g + A\omega_{ref} + \dot{\omega}_{ref} \quad (26)$$

The following (27) is the control strategy considered for disturbance elimination and speed control

$$u = K_1|e|^{1/2}sgn(e) + \omega$$

$$\dot{\omega} = -K_2 sgn(e) \quad (27)$$

where $K_1 and\ K_2$: positive constant respectively

From (26) and (27), the command $T_g$ of a system (23) to tracking the speed reference $\omega_{ref}$ is as

$$T_g = \frac{1}{B}\left[A\omega_{ref} + \dot{\omega}_{ref} - K_1|e|^{1/2}sgn(e) + \omega\right]$$

$$\dot{\omega} = -K_2 sgn(e) \quad (28)$$

### 3.2 Model of Robustness and Uncertainty

Now, let us consider (23) with uncertainties as

$$\dot{\omega}_r(t) = -(A - \Delta A)\omega_r(t) - (B + \Delta B)T_g(t) + d(t) + \zeta(t) \quad (29)$$

given that $\zeta$: any external disturbance

$\Delta$: parametric uncertainty

Now, (29) is reorganized to be

$$\dot{\omega}_r(t) = -A\omega_r(t) - BT_g(t) + d^*(t) \quad (30)$$

$$d^*(t) = -\Delta A\omega_r(t) - \Delta BT_g(t) + d(t) + \zeta(t) \quad (31)$$

*Assumption 1:* Parameters in (22) are uncertain with bounded uncertainties such as

$$J = \bar{J} + \Delta J; K = \bar{K} + \Delta K \quad (32)$$

$$|\Delta J| \le \delta_j; |\Delta K| \le \delta_k$$

unmodeled quantities. Therefore, the SMC (27) will reject the bounded perturbation. It is good to note that the limitation of the system in physical terms and the behavior during operation was considered. As such, the following assumptions were made;

.

Where $\delta$: known bounded positive constant

"-'': denotes a nominal value

$\Delta$: uncertainty

*Assumption 2:* speed and rotor acceleration are bounded as

$$|\dot{\omega}_r| \le \dot{\omega}_r^M \ \&\ |\omega_r| \le \omega_r^M \quad (33)$$

Where $\dot{\omega}_r^M$: maximum value of acceleration

$\omega_r^M$: maximum value of speed

*Assumption 3:* $T_r$ is an unknown turbine torque but bounded as

$$|T_r| \le \delta_T \omega_r^M \quad (34)$$

Where $\delta_T$ : known constant

*Assumption 4:* from 1-3, it can be concluded that the perturbation is bounded as

$$|d^*| \le \delta\omega_r^M \quad (35)$$

At varying wind speed, (28) will ensure robustness to uncertainties like unknown turbine torque and parametric variations.

### 3.3 Performance Evaluation

The evaluation of the controller was obtained via the use of reductions in chattering and drive trainload. Chattering is caused by a large fluctuation of power due to varying wind speeds. Statistically, it is established that approximately 68 percent of the value of a given data set provided that it is normally distributed, lay within a standard deviation ( $\sigma$ ) from the mean ( $\mu$ ) and approximately 95 percent within two[7].

$$Del\ P(\%) = \frac{2\sigma P_e}{P_{e\ nom}} \quad (36)$$

$$Del\ \Omega_r(\%) = \frac{2\sigma\Omega_r}{\Omega_{r\ max}} \quad (37)$$

## 4.0 RESULT AND DISCUSSION

The detailed results obtained for the developed technique, the performance evaluation and the linearized model for the WEC system are presented. Also, the proposed SOSM results in comparison with baseline controller for the WT system is as well presented.

**Table 1: System Parameter**

| Items | Specifications |
|---|---|
| **Synchronous speed (rev/min)** | 1500 |
| **Rated power (kW)** | 2000 |
| **Stator voltage ($V_{rms}$)** | 690 |
| **Rated stator current ($A_{rms}$)** | 1760 |
| **Stator connection** | Star |
| **Pole** | 2 |
| **Rated $V_{\_r}V_{rms}$** | 2070 |
| **Rotor connection** | Star |
| **u** | 0.34 |
| **$R_s$ (mΩ)** | 2.6 |
| **$L_{\sigma s}$(mH)** | 0.087 |
| **$L_m$(mH)** | 2.5 |
| **$R_r'$(mΩ)** | 26.1 |
| **$L_{\sigma r}'$(mH)** | 0.783 |
| **$R_r$ (mΩ)** | 2.9 |
| **$L_{\sigma r}$(mH)** | 0.087 |
| **$L_r$(mH)** | 2.587 |
| **$L_s$(mH)** | 2.587 |
| **$V_{base}$** | 398.4 |
| **$I_{base}$** | 1760 |
| **$I_{\sigma s}$** | 0.12 |
| **$I_{\sigma r}$** | 0.12 |
| **$r_s$** | 0.011 |
| **$r_r$** | 0.012 |
| **$I_m$** | 3.45 |

### 4.1 Control Response

Figure 4. shows the model of the wind speed profile at 8m/s. The effective wind speed of the model is smoother and shows the dynamic nature of wind at a maximum speed of 9.2m/s and minimum speed of 7.5m/s, respectively, as compare to wind speed model at stationary point.

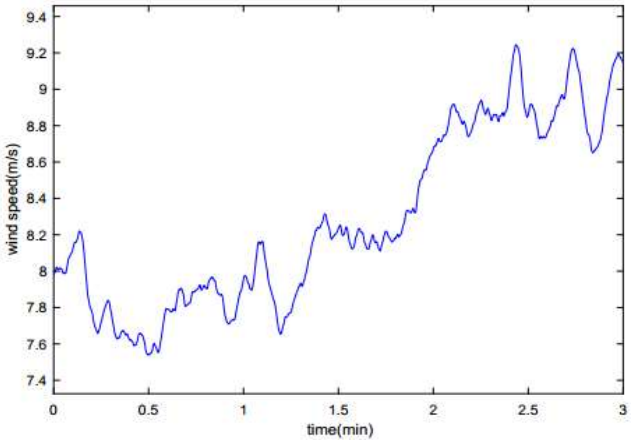


Figure 4: Effective wind speed model

At a wind speed of 8m/s shown in Figure 5, the magnitude of wind is within 6.75% below and above its mean value with less distortion and noise as compared to the baseline controller.

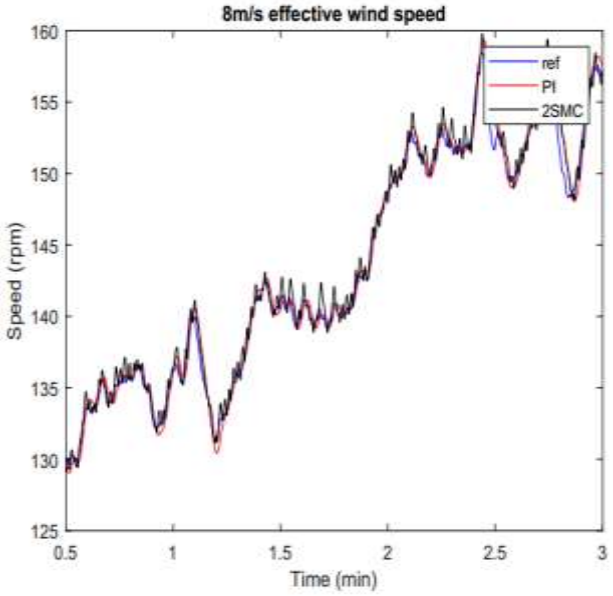


Figure 5: Tracking response of both controllers

In Figure 6, the controller tracks the generator torque with $7.414 \times 10^3$Nm of the nominal value 18554Nm within the interval of 180s. This explains the robustness as well as chattering reduction in SOSM in dynamic-wind speed variation.

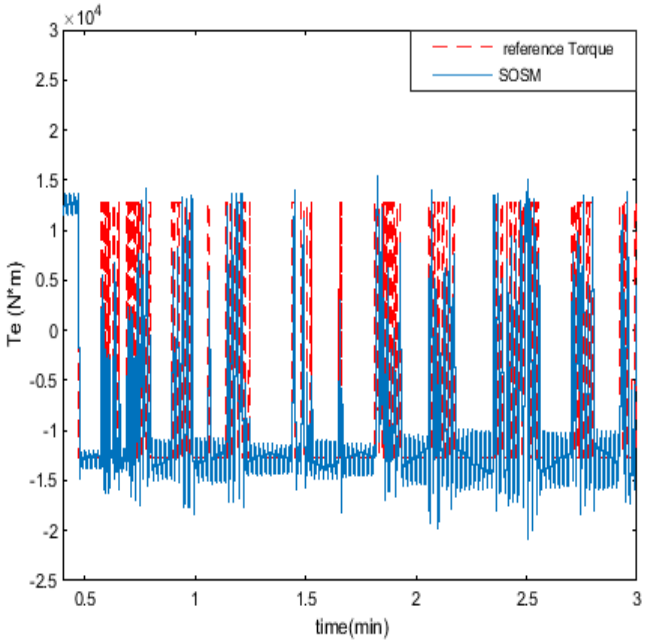


Figure 6: Generator Torque as a Function of Time

Table 2. **Comparison Between SOSM and PI Controller**

| S/N | Comparison Between SOSM and PI Controller | | |
|---|---|---|---|
| | | ***SOSM*** | ***PI*** |
| 1 | $\boldsymbol{\mu P}$(W) | 71,734 | 515,125 |
| **2** | $\boldsymbol{\sigma P}$ (W) | 500,739 | 804,659 |
| **3** | ***Del*** (%) | 75.8449 | 98.2675 |
| **4** | $\boldsymbol{\sigma\Omega_r}$(rad/s) | 49.2189 | 35.3444 |
| **5** | $\boldsymbol{\mu\Omega_r}$(rad/s) | 34.3573 | 55.2102 |
| **6** | ***Del*** (%) | 0.4773 | 0.7684 |

Table 2 shows the summary of the result obtained, a reduction of 500,739W in chattering was obtained for SOSM when compared with PI controller of 804,659W, representing 37.7700% reduction and 35.3444rad/s at a wind speed of 8m/s.

## 5.0 CONCLUSION

This research work has presented the techniques for chattering reduction in SOSM control systems. The research shows the use of the classical baseline controller as a control strategy for the WT system degrades over time with inefficient tracking performance due to abrupt changes in wind speed. The technique tracking performance was remarkable, with 37.7700% in chattering reduction compared to PI Controller and 35.3444rad/s drive train load. However, the inconsistence from wind resulted the increase in drive train load. Thus, the work shows the effectiveness of SOSM control techniques in achieving a better tracking performance of WT systems with significant chattering reduction. The SOSM was shown to outperform the baseline PI controller when implemented on a DFIG-based WT system.

## REFERENCES

[1] Adel M, Ahmed K.T, Ibrahim H and Benguenane R,(2016). Implementation of Sliding Mode Control System for Generator and Grid Sides Control of Wind Energy Conversion System. IEEE transactions on sustainable energy. doi: 10.1109/TSTE.2016.2537646.

[2] Alex K, Katherine D and Kathy A, (2015). Introduction to DFIG for Wind Power Application. Department of Earth, Atmospheric and Planetary Science (EAPS) MIT, 259-278.

[3] Alhazmi M.M, (2015). Modelling of Doubly-Fed Induction Generator using MATLAB/SIMULINK. Master's thesis, California state university Los Angeles

[4] Bayat M.M and Torun Y, (2017). Modelling and Linearization of DFIG Based Wind Turbine. European Scientific Journal July 2017 /SPECIAL/ edition ISSN: 1857 – 7881 (Print) e - ISSN 1857- 7431, 158-168.

[5] Chinmaya and Singh (2019). Modelling and experimental analysis of grid-connected six-phase induction generator for variable speed wind energy conversion system Electric Power Systems Research 166 pp 151–162

[6] Ebrahimkhani S, (2016). Robust Fractional Order Sliding Mode Control of Doubly-Fed Induction Generator (DFIG)-based Wind Turbines. ISA Transactions, 1-12. http://dx.doi.org/10.1016/j.isatra.2016.03.003

[7] Gosk A, (2011). Model predictive control of a wind turbine. Master's thesis, Technical University of Denmark.

[8] Krim Y, Abbes D, Krim S and Mimouni M.F, (2017). Classical Vector, First-Order Sliding Mode and High-Order Sliding-Mode Control for A Grid-Connected Variable Speed Wind Energy Conversion System: A Comparative Study. Wind Engineering 1–22: DOI: 10.1177/0309524X17723202

[9] Muhammad A.S., Ai-jun L., Bing H., Yu W., and Bojian L., (2019). "Comparative Analysis of Neural-Network and

Fuzzy Auto-Tuning Sliding Mode Controls for Overhead Cranes under Payload and Cable Variations" Journal of Control Science and Engineering, Article ID 1480732, https://doi.org/10.1155/2019/1480732, pp1-13

[10] Petersson A, (2005). Analysis, Modelling and Control of Doubly-Fed Induction Generator for Wind Turbine. PhD thesis, Chalmers University of Technology Sweden

[11] Pantea A, A. Yazidi, F. Betin, M. Taherzadeh, S. Carriere, H. Henao and G. A. Capolino (2018a)." Fault - Tolerant Control of a Low Speed Six-Phase Induction Generator for Wind Turbines" IEEE Transactions on Industrial Electronics, DOI 10.1109/TIA.2018.2870385

[12] Pantea A, A. Yazidi, F. Betin, M. Taherzadeh, S. Carriere, H. Henao and G. A. Capolino (2018b)." Fuzzy logic Control of a Low-Speed Six-Phase Induction Generator for Wind Turbines" IEEE Transactions on Industrial Electronics, DOI 10.1109/TIA.2018.2870385

[13] Patnaik R.K and Dash P.K, (2016). Fast Adaptive Back-Stepping Terminal Sliding Mode Power Control for Both the Rotor-Side as Well as Grid-Side Converter of the Doubly Fed Induction Generator-Based Wind Farms. IET Renew. Power Gener., doi: 10.1049/iet-rpg.2015.0286 pp. 1–13.

[14] Shehu A.F, Abubakar A.S, Musayyibi S. and Idris K. (2019). Doubly Fed Induction Generator Based Wind Energy Conversion System: A Review. Journal of Science Technology and Education 7(3), ATBU Bauchi pp 145-150

[15] Si and Liu. (2015). Model predictive control for DFIG-based wind power generation under unbalanced network conditions. Paper presented at the Control Conference(CCC), 2015 34th Chinese.

[16] Sun H, Han Y and Zhang L, (2018). Maximum Wind Power Tracking of Doubly Fed WindTurbine System Based on Adaptive Gain Second-Order Sliding Mode. Journal of Control Science and Engineering Volume 2018, Article ID 5342971, doi.org/10.1155/2018/5342971, 11 pages